LIP-STUDENTS-25-25

Search for Dark Higgs with SND@LHC

Rodrigo Castanheira[1,a]

[1] *Instituto Superior Técnico*

Project supervisors: Cristóvão Vilela and Nuno Leonardo

November 25, 2025

Abstract. Despite the success of the theory of the Standard Model (SM), there are multiple open questions that require Beyond the Standard Model (BSM) extensions. The Scattering and Neutrino Detector at the Large Hadron Collider (SND@LHC) is a detector designed for the study of collider neutrinos and capable of also studying Feebly Interacting Particles (FIPs). Following in the footsteps of previous work, this article aims to analyze possible FIP decays into muon pairs through the Dark Higgs, validating and optimizing multiple selection metrics of the signal measured at the SND@LHC. After the analysis of single muon and neutrino backgrounds, selection cuts were devised for their elimination whilst minimizing signal reduction. Through application of these metrics, $N_{5\sigma} = 106$ counts are needed for background-only exclusion at 5σ, without taking signal efficiency into account and for a run with an abnormally inefficient Veto system.

Keywords: Feebly Interacting Particles, Dark Higgs, Signal Analysis, Background-Only Exclusion

1 Introduction

1.1 The Dark Higgs

The problem of Dark Matter (DM) cannot be explained by the Standard Model of Particle Physics. There are multiple BSM particle candidates of DM, some of which are Feebly Interacting Particles, which have very weak interactions with the SM particles. This work will focus on a scalar portal, involving a scalar particle (spin 0) that only interacts with the SM through mixing with the SM Higgs boson, an interaction which is quantified by a mixing angle. This addition to the SM is simple and allows direct detection through interaction with the SM Higgs.

The chosen scalar portal is the Dark Higgs (DH), and a real scalar field h' is added to the SM scalar potential, which can be written as [1, 2]:

$$V(|H|, h') = \mu_H^2|H|^2 - \frac{1}{4}\lambda_H|H|^4 + \mu'^2 h'^2 - \mu_3' h'^3 - \frac{1}{4}\lambda' h'^4 - \mu_{12}' h'|H|^2 - \varepsilon h'^2|H|^2 \quad (1)$$

where H is the Higgs doublet, ε is the coefficient of the quartic interaction that serves as the portal in this model, μ_H and μ' are the Higgs and DH mass parameters, respectively, and the rest of the coefficients are coupling constants.

H and h' are interaction eigenstates, so after finding the minima of the new potential and diagonalizing the mass terms, the resulting physical eigenstates are the SM Higgs boson h and the DH boson ϕ. In this work, a phenomenological parametrization is considered, and the Lagrangian of the DH boson is [2]:

$$\mathcal{L}_\phi = -\frac{1}{2}m_\phi^2\phi^2 - \sin\theta\frac{m_f}{v}\phi\bar{f}f - \lambda v h\phi\phi + \dots \quad (2)$$

where m_ϕ is its mass, θ is the mixing angle with the Higgs, f is a massive fermion with mass m_f, λ is the trilinear coupling and v is the Higgs vacuum expectation value. The cubic and quartic interactions between h and ϕ have been omitted.

For presently viable DH parameters, the predominant methods of DH production are meson decays. In decreasing order of dominance, they are:

- B meson decays dominated by the $b \to s\phi$ process, involving an $(u, c, t)-W$ loop dominated by top quark contribution:

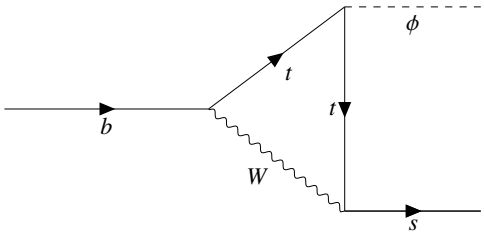

Figure 1. Feynman diagram for $b \to s\phi$ with a top quark-W loop in the B meson decay involved in Dark Higgs production. Adapted from Ref. [1].

- K meson decays dominated by the $s \to d\phi$ process, involving an $(u, c, t)-W$ loop dominated by top quark contribution:

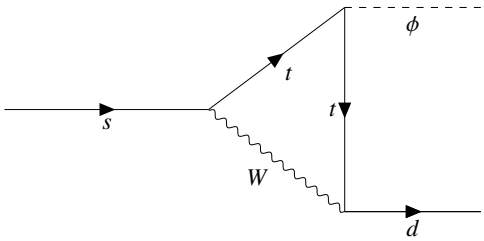

Figure 2. Feynman diagram for $s \to d\phi$ with a top quark-W loop in the K meson decay involved in Dark Higgs production. Adapted from Ref. [1].

[a] e-mail: rodrigo.f.castanheira@tecnico.ulisboa.pt

- Other light meson decays, such as $\eta' \to \eta\phi$, $\eta \to \pi^0\phi$ and $\pi^\pm \to e\nu\phi$.

The hierarchy of these processes can be seen from their branching fractions: $B(B \to \phi) \gg B(K \to \phi) \gg B(\eta, \pi \to \phi)$. This is the case because the DH inherits couplings of the SM Higgs.

As seen in Figure 3, the possible DH decay modes depend on the chosen mass of the DH boson. Because the desired DH decay is to a muon-antimuon pair, a DH mass of $m_\phi = 251.2\,\text{MeV}$, greater than twice the muon mass but lesser than twice the pion mass, is chosen.

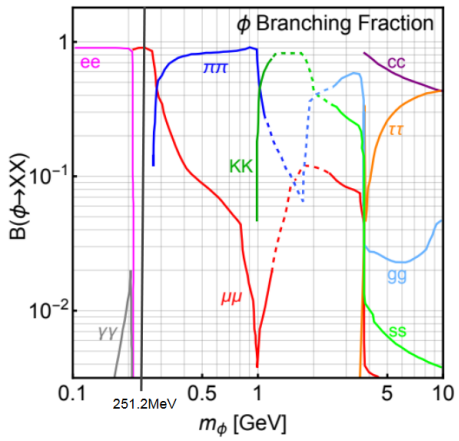

Figure 3. Branching fractions of the DH decay to SM particles as a function of the DH mass. The chosen mass is denoted by a vertical line. From Ref. [1].

1.2 SND@LHC

The Scattering and Neutrino Detector at the LHC is a stand-alone experiment for the study of neutrinos produced in Large Hadron Collider (LHC) collisions. It is located 480 meters downstream of the ATLAS detector, approximately collinear with the collider beams (Figure 4). Charged particles produced by the LHC are diverted by the LHC magnets and other neutral particles are stopped by 100 meters of underground material, so the particle background is severely reduced. Despite the main purpose of the detector being the study of collider neutrinos, its distance from the collision point and muon detection system are very advantageous for FIP research such as the study of the aforementioned DH decay into a dimuon pair.

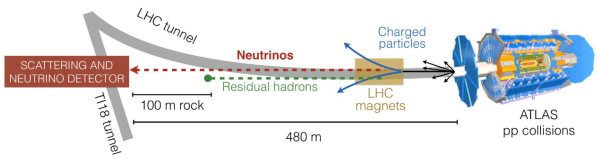

Figure 4. Schematic of the SND@LHC detector and the trajectory of charged particles and neutral particles from the ATLAS interaction point. From Ref. [3].

There are three main components to the detector (Figure 5): the Veto System, the Electromagnetic Calorimeter and the Hadronic Calorimeter.

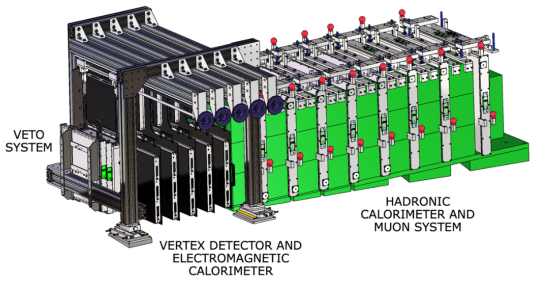

Figure 5. Scheme of the full SND@LHC detector. From Ref. [4].

The Veto System detects the passage of charged particles through the front of the detector, using scintillator bar planes that are read by silicon photomultipliers. This way, charged particles that make it through the underground material and enter the detector can be distinguished from those produced inside the detector.

The Electromagnetic Calorimeter consists of five walls composed of emulsion bricks filled with emulsion films, alternated with tungsten plates. These high density plates induce a large number of particles that are then recorded by the films with high spatial resolution, which can be revealed later to provide the trajectory and nature of the particle interactions. Between the walls there are scintillating fiber (SciFi) trackers that are used for temporal and spatial information, as well as measuring the energy of induced electromagnetic showers. Due to the interaction lengths of tungsten, electromagnetic showers can be contained in this section of the detector, while hadronic showers cannot.

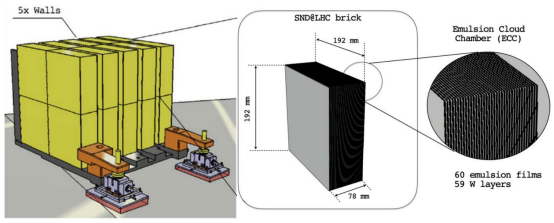

Figure 6. Scheme of the Electromagnetic Calorimeter of the SND@LHC, composed of the Emulsion Target and Scintillating Fiber Trackers. From Ref. [5].

The Hadronic Calorimeter consists of eight planes, each composed of scintillating bars. The first five planes only have horizontal bars and are called Upstream (US), while the last three have both horizontal and vertical bars and are called Downstream (DS). This subsystem allows the measurement of the aforementioned hadronic showers, as well as the detection of the passage of muons.

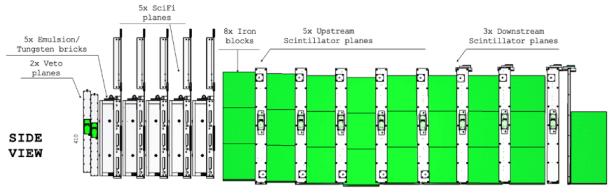

Figure 7. Scheme of the Hadronic Calorimeter and Muon System of the SND@LHC. From Ref. [6].

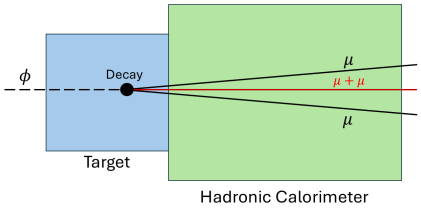

Figure 8. Scheme of the dimuon tracks registered by the detector. If the opening angle was bigger than the sensibility, the tracks would be resolved as represented in black. As it is smaller, the track is collinear, represented in red. Adapted from Ref. [1].

2 Backgrounds and Dimuon Signal

For this analysis, only $\phi \to \mu^- \mu^+$ decays inside the Electromagnetic Calorimeter region will be considered, so that the scintillating fiber system can be used. The backgrounds to be excluded consist of the muons coming from outside the detector and the products of neutrino interactions inside the detector.

2.1 Opening Angle

The relativistic momentum in the laboratory frame of each of the muons created in the DH decay is given by [1]:

$$\begin{aligned} p_1' &= \left(\frac{\beta\gamma M}{2} + A\cos\theta_z, A\sin\theta_z\right), \\ p_2' &= \left(\frac{\beta\gamma M}{2} - A\cos\theta_z, -A\sin\theta_z\right), \\ A &= \sqrt{\frac{M^2}{4} - m^2} \end{aligned} \tag{3}$$

where the first component of each momentum denotes the momentum in the DH propagation direction, the z axis, and the second denotes the transverse momentum. v is the center of momentum velocity, $\beta = v/c$, $\gamma = 1/\sqrt{1-\beta^2}$ and θ_z is the polar angle with the z axis.

For the muon tracks to be discernible in the Hadronic Calorimeter, due to its geometry, the opening angle must be at least 10^{-3} rad. Calculating the opening angle α between the two muon tracks after the decay:

$$\alpha = \arccos \frac{p_1' \cdot p_2'}{|p_1'||p_2'|} \tag{4}$$

it can be concluded that for the chosen DH mass and for the observed DH momentum, the opening angle is smaller than the sensibility. Thus, a singular track of the overlapping dimuon pair will be considered for future analysis (Figure 8).

2.2 QDC Likelihood

Each US hit has a Charge-to-Digital Converter (QDC) value that allows for the quantification of the deposited energy.

Probability density functions (PDFs) are generated for each US plate, one for the dimuon signal, and one for the muon background. After calculating the most probable values (MPV) for each PDF, each PDF is shifted by the difference between the average of MPVs and its own MPV. All US plane PDFs are then summed, for both dimuon and muon distributions.

The QDC likelihood ($NLLR$) is then calculated as follows:

$$NLLR = \sum_i \ln(P_1(A_i)) - \ln(P_2(A_i)) \tag{5}$$

where A_i are the QDC values measured at each of the US planes, P_1 is the muon PDF and P_2 is the dimuon PDF [1].

If the QDC likelihood is larger than the chosen threshold, it is more similar to a muon background, otherwise, it is closer to a dimuon signal.

2.3 Reconstructed Track

A straight line track of the path of the muons inside the detector can be reconstructed from the hits in the DS planes and further extrapolated to earlier components of the detector (Figure 9). This is done mathematically using a point in the recognized track and the corresponding momentum at that point. This reconstruction is imperfect and can deviate from the detected hits. Events that do not have enough information to recognize a muon track are not considered for the analysis.

2.4 Backgrounds

The track of a single muon passing through the detector is identical to the track of a dimuon pair due to the previously mentioned collinearity. There are methods of distinguishing between the two, such as the QDC likelihood or registering a hit in the Veto, but the latter has an inefficiency of 2.5×10^{-6} [7], so muons passing through the Veto constitute a relevant background.

Muon neutrinos pass through the Veto as well without registering a hit, so the production of a muon from the

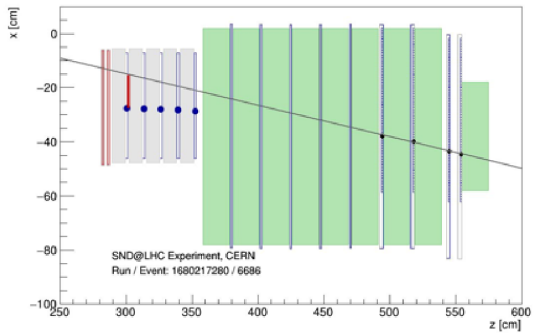

Figure 9. Reconstructed muon track based on the DS plane hits. The red line represents the maximum deviation between the track and the detected hits. From Ref. [1].

interaction with the detector can be similar to the desired signal if the other products are not detected. Both of these backgrounds will be taken into account henceforth.

3 Signal Selection

Based on the dimuon signal analysis, multiple selection cuts are devised to eliminate the most background events whilst keeping the best possible signal selection efficiency. These cuts are applied to SND@LHC data that was converted into a format that contains parameters crucial for the selection. The sequentially applied cuts, in the corresponding order, are the following:

1. To eliminate events that barely pass through the detector or that enter from the sides, the track extrapolation is required to coincide with the Veto x and y limits ($x \in [-47, -8]$ cm, $y \in [15.5, 54.5]$ cm), taking 2.5 cm from the edges ($x \in [-44.5, -10.5]$ cm, $y \in [18, 52]$ cm) to ensure exclusion of border hits.

2. Reconstructing the tracks from the DS hits alone makes them sometimes unreliable, so the square of the maximum distance from the reconstructed track to the registered hits is taken to be nonzero and limited from above to prevent unphysical track reconstruction ($(0 < d^2 \leq 3)\,\text{cm}^2$).

3. The total number of US hits must be less than 10 to exclude hadronic showers originated by neutrino interactions.

4. To ensure that hadronic showers are eliminated, a further limit of two hits per US plane is placed (whilst allowing for simultaneous hits on two bars if the muon passes between them).

5. The polar angle (angle between the track and the z axis) is limited to guarantee that the incoming particles were produced in the LHC collisions and prevent diagonal entrances in the detector ($\theta < 86.9$ mrad).

6. To eliminate electromagnetic showers from neutrino interactions, the number of total hits throughout the SciFi trackers is taken to be less than 96.

7. The QDC likelihood of the event is used to discern between dimuon signal and muon background, with a threshold of -7.5 (the event is considered signal if the likelihood is smaller than the threshold).

8. As the DH is a neutral particle and only decays inside the detector, the event is required to register no Veto hits, which eliminates single muons entering the detector.

Application of these cuts to a $0.6\,\text{fb}^{-1}$ sample of SND@LHC data (which is referred to as run 5000) yields the preliminary results in Table 1.

Run 5000 ($N = 4.5 \times 10^7, L = 0.6\,\text{fb}^{-1}$)	
Applied Cuts	Surviving Events (%)
Veto XY limits	29.609 ± 0.007
Maximum distance squared	3.252 ± 0.003
Total US hits	3.252 ± 0.003
US hits per plane	2.556 ± 0.002
Polar angle	1.241 ± 0.002
Total SciFi hits	1.241 ± 0.002
QDC likelihood	$(4.281 \pm 0.307) \times 10^{-4}$
Veto hits	0 ± 0

Table 1. Surviving event percentages resulting of cut application to real data (run 5000).

The uncertainty of the surviving events is given by:

$$\sigma = \sqrt{\frac{\varepsilon(1-\varepsilon)}{Y}} \times 100\%, \varepsilon = \frac{X}{Y} \tag{6}$$

where X are the surviving counts, Y is the number of counts in the sample and ε is the surviving fraction of counts.

4 Background Estimation

4.1 Single Muon Background

To estimate the single muon background after all cuts have been applied (in the signal region), the ABCD method is employed [1]. This method consists of the selection of two sufficiently uncorrelated selection cuts to delimit four regions, of which three are background regions (B, C and D) and one is the signal region (A) (Figure 10). The considered cuts for muon background estimation are the QDC likelihood and the hits in the Veto.

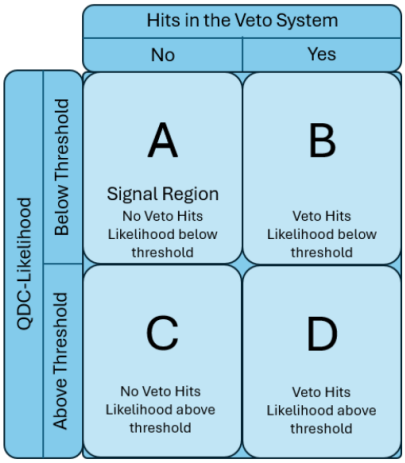

Figure 10. Diagram for the ABCD method regions chosen for data analysis. From Ref. [1].

The lack of correlation between the selected cuts can be expressed as a relation between the background counts in each of the regions [1]:

$$\frac{N_A^{bkg}}{N_B^{bkg}} = \frac{N_C^{bkg}}{N_D^{bkg}} \tag{7}$$

However, due to the properties of the DH signal, the background regions have a negligible amount of signal events in relation to the muon background ($N_i \approx N_i^{bkg}, i = B, C, D$), and thus, from Equation 7, an estimation for the signal region background can be made:

$$N_A^{bkg} = \frac{N_C^{bkg}}{N_D^{bkg}} N_B^{bkg} \approx \frac{N_C}{N_D} N_B \tag{8}$$

The application of the ABCD method to the same run 5000 data sample (that yielded no surviving counts after successive application of all selection cuts) is shown in Table 2.

Run 5000 ($N = 4.5 \times 10^7, L = 0.6\,\text{fb}^{-1}$)	
Region	Counts
B	194
C	487
D	562473

Table 2. Surviving counts for each region of the ABCD method, in run 5000.

Using Equation 8, the estimated single muon background for this $0.6\,\text{fb}^{-1}$ sample, in the signal region, is $N_\mu^{bkg} \approx 0.168 \pm 0.014$, where the uncertainty given by:

$$\delta N_\mu^{bkg} = \frac{\sqrt{N_B N_C (N_B + N_C)}}{N_D} \tag{9}$$

4.2 Neutrino Background

Because neutrinos are neutral particles and do not register a hit in the Veto, the ABCD Method cannot be used because the last cut does not apply. However, it is still possible to make an initial estimation based on a Monte Carlo (MC) neutrino simulation sample.

Through successive application of the previously established cuts, excluding the Veto hit cut, to a $30\,\text{fb}^{-1}$ MC neutrino sample, the surviving percentages in Table 3 are obtained, with uncertainties given by Equation 6.

Neutrino MC ($N = 10878, L = 30\,\text{fb}^{-1}$)	
Applied Cuts	Surviving Events (%)
Veto XY limits	76.99 ± 0.40
Maximum distance squared	1.89 ± 0.13
Total US hits	1.49 ± 0.12
US hits per plane	0.864 ± 0.089
Polar angle	0.864 ± 0.089
Total SciFi hits	0.855 ± 0.088
QDC likelihood	0.00919 ± 0.00919

Table 3. Cuts applied to a neutrino MC simulation and the surviving percentages for each cut.

From the 10878 neutrinos simulated, only one event survives, so the estimated neutrino background for $30\,\text{fb}^{-1}$ is $N_\nu^{bkg} = 1 \pm 1$.

5 Results and Conclusions

5.1 Extrapolated Results

Extrapolating the results to $200\,\text{fb}^{-1}$, which correspond to approximately SND@LHC's integrated luminosity from 2022 to 2024, $N_\mu^{bkg} = 56.00 \pm 2.67$ counts are obtained for the single muon background and $N_\nu^{bkg} = 6.67 \pm 6.67$ for the neutrino background.

Through a hypothesis test with the 5σ threshold p-value, $p_{5\sigma} = 2.87 \times 10^{-7}$, the smallest number of counts that excludes the hypothesis that there are only background events, at a 5σ significance, is $N_{5\sigma} = 106$.

Moreover, the selection cuts also have a certain efficiency ε_{sig} when applied to the signal, which can be determined through the analysis of DH MC simulations. When taking that efficiency into account, $N_{5\sigma}/\varepsilon_{sig}$ counts would be needed for background-only exclusion.

5.2 Conclusions and Future Work

In conclusion, the verification and optimization of the previously developed methods of data selection in search of the Dark Higgs was successful. The SND@LHC is an experiment with great potential for FIP studies and the devised selection cuts are very efficient at eliminating the background. Despite the $N_{5\sigma} = 106$ counts needed for background exclusion being promising, these results were obtained from a run with an abnormally large Veto inefficiency [1], so the counts required for a data set with the usual efficiency could be lower, even after taking into account the signal selection efficiency.

In future work, the first step would be to calculate the signal selection efficiency using DH MC simulations. Applying this analysis to a larger set of SND@LHC data and

optimizing the cuts to the larger sample would also lead to more accurate results, as extrapolation would be unnecessary. Other DM particle models could be considered, as long as the dimuon decay is still the most relevant.

Acknowledgements

I would like to thank my supervisors, Cristóvão Vilela and Nuno Leonardo, for their constant and invaluable guidance and support during every step of this internship. Thank you also to Guilherme Soares for his advice and assistance during the project, and to Henrique Santos for establishing the bases for this work. I am grateful for my internship colleagues, João Galhardo, João Goulão and Rafael Fernandes for their help and positive learning environment. Lastly, thank you to LIP and their Summer Internship program for the incredible opportunity and the enriching learning environment.

References

[1] H. Santos, *Searching for Beyond the Standard Model particles decaying to muon pairs with SND@LHC*, https://cds.cern.ch/record/2921745 (2024), CERN-THESIS-2024-307

[2] J.L. Feng, I. Galon, F. Kling, S. Trojanowski, Physical Review D **97** (2018)

[3] F. Alicante (2023), https://cds.cern.ch/record/2876147

[4] A. Iuliano, preprint (2023), https://doi.org/10.48550/arxiv.2308.00097

[5] C. Yoon, *High-energy neutrinos at LHC with SND@LHC* (2022), https://cds.cern.ch/record/2825489/files/RencontresVietnam2022_yoon.pdf

[6] M. Komatsu, for the SND@LHC Collaboration, Physical Sciences Forum **8**, 48 (2023)

[7] SND@LHC Collaboration, Phys. Rev. Lett. **131**, 031802 (2023)